Construction of a consistent YAC contig for human chromosome region 3p14.1

Bardenheuer, W.; Michaelis, S.; Lux, A.; Vieten, L.; Brocker, F.; Julicher, K.; Willers, C.; Siebert, R.; Smith, D. I.; vanderHout, A. H.

Published in:
Genome Research

DOI:
10.1101/gr.6.3.176

RESEARCH

Construction of a Consistent YAC Contig for Human Chromosome Region 3p14.1

Walter Bardenheuer,[1] Susanne Michaelis,[1] Andreas Lux,[1] Lydia Vieten,[1] Frank Bröcker,[1] Knut Jülicher,[1] Christoph Willers,[1] Reiner Siebert,[1] David I. Smith,[2] Annemarie H. van der Hout,[3] Charles Buys,[3] Jochen Schütte,[1,4] and Bertram Opalka[1,4]

[1]Innere Klinik und Poliklinik (Tumorforschung), Universitätsklinikum Essen, Westdeutsches Tumorzentrum, 45122 Essen, Germany; [2]Institute of Molecular Biology, Wayne State University, Detroit, Michigan 48201; [3]Department of Medical Genetics, University of Groningen, Groningen, Netherlands

Chromosomal deletions and translocations of human chromosome region 3p14 are observed in various human malignancies and suggest the existence of a tumor suppressor gene locus within this region. Tumors most frequently affected by these aberrations are small-cell lung cancer and renal-cell carcinoma. In continuation of our previously published YAC contig of chromosome region 3p14.2–p14.3, we report here on the construction of a YAC contig of at least 11 Mb that consisted of 171 YACs and covers the entire subregion 3p14.1. This contig includes the t(3;8) breakpoint of a hereditary renal-cell carcinoma localized in 3p14.2 and extends into human chromosome region 3p12–p13. It defines the order of 34 DNA probes in relation to reference markers D3S6 and D3S30 as well as the human protein tyrosine phosphatase-γ gene. For 31 DNA probes we identified nonchimeric YACs by fluorescence in situ hybridization. The minimal tiling pathway consists of 16 yeast artificial chromosomes. As a prerequisite for identification of a putative tumor suppressor gene within this region, this contig renders human chromosome region 3p14.1 accessible to gene isolation.

The short arm of human chromosome 3 is frequently affected by chromosomal deletions and translocations as determined by cytogenetical and loss-of-heterozygosity (LOH) studies in many types of human tumors. Among these are small-cell (SCLC) and non-small-cell lung cancer (NSCLC) (Brauch et al. 1987; Kok et al. 1987; Naylor et al. 1987; Yokota et al. 1987; Johnson et al. 1988; Becker and Sahin 1989; Mori et al. 1989; Rabbitts et al. 1989; Weston et al. 1989; Hibi et al. 1991, 1992; Yokoyama et al. 1992), renal-cell carcinoma (RCC) (Zbar et al. 1987; Bergerheim et al. 1989; Morita et al. 1991), head and neck carcinoma (Latif et al. 1992), breast cancer (Devilee et al. 1989; Sato et al. 1991), ovarian cancer (Whang-Peng 1984; Trent et al. 1985; Ehlen and Dubeau 1990), cervix carcinoma (Yokota et al. 1989; Kohno et al. 1993; Jones et al. 1994), and testis carcinoma (Lothe et al. 1989).

Functional analysis and LOH studies may suggest the existence of one or more tumor suppressor gene loci in human chromosome region (HCR) 3p13–p21.1. In particular, HCR 3p14 contains the translocation breakpoint t(3;6) associated with hematological malignancies (Markkanen et al. 1987), as well as the translocation breakpoints t(3;6) in 3p14.1 (Kovacs et al. 1989; van den Berg et al. 1995) and t(3;8) in 3p14.2 (Cohen et al. 1979; Wang and Perkins 1984; Drabkin et al. 1985) that are associated with hereditary RCC. Although two of these breakpoints were cloned recently (Boldog et al. 1993; Smith et al. 1993), no tumor suppressor gene close to them has been published to date. Recently, clustering of terminal deletion breakpoints in nonpapillary RCC was reported (Wilhelm et al. 1995); in this study, the most distal breakpoint mapped to HCR 3p14.1–p14.2 between markers D3S1285 and D3S1300; this region contains the t(3;8) translocation breakpoint found in a hereditary RCC. In functional analyses, HCR 3p12–p14 but not 3p11–q24 showed suppression of tumorigenicity of an RCC cell line (Sanchez et al. 1994). In addition, a bladder carcinoma cell line whose tumorigenicity was suppressed by the fusion with a cell line showing hemizygous loss of chromosome 3 regained tumorigenicity after loss of chro-

[4]Corresponding authors.
E-MAIL bertram.opalka@uni-essen.de; FAX +49 201-723-5925/2020.

6:176–186 ©1996 by Cold Spring Harbor Laboratory Press ISSN 1054-9803/96 $5.00

mosome 3p material with the smallest region of deletion ascribed to HCR 3p13–21.2 (Klingelhutz et al. 1992).

As the marker density increased and yeast artificial chromosome (YAC) libraries became available in recent years, a contig covering almost the entire human chromosome 3 (Gemmill et al. 1995), as well as subcontigs for HCR 3p14.2–p14.3 (Michaelis et al. 1995) and the distal part of 3p14.1 (Boldog et al. 1994) have been published. In this paper we describe the constuction of a YAC contig for HCR 3p14.1 by PCR-based analysis, Southern blot, and Alu-fingerprint analysis. This contig contains at least 11 Mb of DNA. It includes the RCC t(3;8) translocation breakpoint localized in 3p14.2 and its most proximal probes map to HCR 3p12–p13. This contig defines the order of 24 previously localized "sequence-tagged sites" (STSs) (Bardenheuer et al. 1994) and 10 new DNA probes in relation to the human protein tyrosine phosphatase-γ (HPTPγ) gene and reference markers D3S6 and D3S30. Thus, it may provide a valuable tool for the identification and analysis of expressed sequences within this putative tumor suppressor gene region.

RESULTS

Analysis of 3p14.1-specific YACs

Twenty-five of the 39 DNA probes used in this study for the isolation of YACs have been described previously (Michaelis et al. 1995). In addition, seven microsatellite markers, three reference markers, two YAC end probes, one Alu-PCR product, and the gene for HPTPγ were included in the contig. YAC clones were identified by defining the DNA probe content of the CEPH YAC and Mega-YAC libraries (Bardenheuer et al. 1994). For the 39 DNA probes analyzed in this study, a total of 182 YACS were found, 171 of which could be assembled into a contig. The contig contains 37 of the 39 probes analyzed. Characteristics and DNA probe content of individual YACs are summarized in Table 1.

The average sizes of the YACs were 500 kb ranging from 150 to 1770 kb for YAC coordinates 1A1 to 735H12 and 1400 kb ranging from 90 to 2500 kb for coordinates 736H1 to 984H12 (Mega-YAC library). FISH analyses of 76 YACs revealed a frequency of chimerism of 41% (Table 1).

Construction of a YAC Contig for HCR 3p14.1

Analysis of the DNA probe content of YACs allowed the identification of overlapping YAC clones. For each DNA probe, an average of 9.2 YACs (range 1–23) was identified. By inclusion of Alu-fingerprint analysis of three YACs, it was possible to construct a contig for HCR 3p14.1 that contains reference markers D3S6 and D3S30, the HPTPγ gene, and 34 DNA probes. The entire contig covers an estimated size of >11 Mb of DNA (Fig. 1). The estimation of the size of the contig was performed by aligning nonoverlapping, nonchimeric YACs and thus gives the minimum size of the region of interest.

The distal boundary of the contig is marked by STS D3S1388 and 1A2 that map distal to the RCC t(3;8) translocation breakpoint in HCR 3p14.2. The most proximal STS in the contig—D3S1405—maps to HCR 3p13 and is localized distal to the distal boundary of the U2020 homozygous deletion in 3p12–p13. Thus, the contig completely covers HCR 3p14.1. A minimal tiling pathway for HCR 3p14.1 as defined in this study can be assembled with 16 of the 171 YACs (Fig. 1).

DISCUSSION

Structural and functional analyses in many human tumor types have suggested that HCR 3p14 contains a putative tumor suppressor gene region (Hibi et al. 1992). The 3p14.1-specific YAC contig presented here, together with our previous report on a 3p14.2–14.3-specific contig (Michaelis et al. 1995) completes our efforts to construct a YAC contig of the entire putative tumor suppressor gene region 3p14. In particular, this contig completes the work of our group to obtain a high-density STS map of HCR 3p14 as well as the availability of a large number of nonchimeric YACs for functional analyses and expression mapping.

The assembly of this contig was possible owing to the availability of 3p14.1-specific STSs derived from a 3p14-specific microdissection library (Bardenheuer et al. 1994). With the redundance of YAC clones for each DNA probe shown here, the order of the probes should be reliable.

The contig presented here is in accordance with the corresponding region of the chromosome 3 contig published by Gemmill et al. (1995). Interestingly, Gemmill et al. (1995) described one Alu fingerprint that links YACs 892d2 and 178a3, with YAC 258b7 covering the region but not containing the Alu fingerprint. In our study, probe D3A1217 links all of the three above-mentioned YACs and therefore gives a re-

Table 1. DNA probe/reference marker content of YACs

YAC	Size (kb)	Localization (by FISH)	Chimeric	DNA probe content
65E7	620	3p14	–	D3S1388(IIIB5)/1A2/D3S1401-(IVH10)/D3S1391(IF8)
74B2	440	no signal	?	1A2
621H4	460	17q or 18q	+	1A2
171B1	640	3p14	–	D3S1388(IIIB5)/1A2/D3S1401-(IVH10)/D3S1391(IF8)/D3S1397-(IVA6)
850A6	**1300**	**3p14**	**–**	**D3S3155(BE758-6)/D3S1388 (111B5)/1A2/D3S1401(IVH10)/ D3S1391(IF8)/D3S1397(IVA6)**
743b3	**1700**	**N.D.**	**N.D.**	**HPTPγ (phosphatase gamma)**
130H11	**220**	**3p14**	**–**	**3B6**
143C5	N.D.	3p14 + G/D-group	+	3B6
880F2	N.D.	N.D.	N.D.	3B6
959h4	**1160**	**N.D.**	**N.D.**	**3B6/D3S1394(IIIE12)**
326F12	350	3p14 + C-group	+	D3S1394(IIIE12)
161G11	N.D.	N.D.	N.D.	D3S1394(IIIE12)
166G8	470	3p13–p14	–	D3S1394(IIIE12)
248A5	N.D.	3p14 + C-group + D-group	+	D3S1394(IIIE12)
288H1	N.D.	N.D.	N.D.	D3S1394(IIIE12)
633e4	N.D.	N.D.	N.D.	D3S1394(IIIE12)
734h8	370	N.D.	N.D.	D3S1394(IIIE12)
746e6	890	N.D.	N.D.	D3S1394(IIIE12)
761g4	1020	N.D.	N.D.	D3S1394(IIIE12)
784f12	1380	N.D.	N.D.	D3S1394(IIIE12)
807c10	N.D.	N.D.	N.D.	D3S1394(IIIE12)
934f8	N.D.	N.D.	N.D.	D3S1394(IIIE12)
927el	1760	N.D.	N.D.	D3S1394(IIIE12)/D3S1400(IVH1)
858a8	1090	N.D.	N.D.	D3S1394(IIIE12)/D3S1400(IVH1)
807e10	1210	N.D.	N.D.	D3S1394(IIIE12)/D3S1400(IVH1)
770h8	**N.D.**	**N.D.**	**N.D.**	**D3S1394(IIIE12)/D3S1400(IVH1)**
933d5	N.D.	N.D.	N.D.	D3S1394(IIIE12)/D3S1400(IVH1)
965h3	N.D.	N.D.	N.D.	D3S1394(IIIE12)/D3S1400(IVH1)
977c8	1690	N.D.	N.D.	D3S1394(IIIE12)/D3S1400(IVH1)
725A5	900	N.D.	N.D.	D3S1394(IIIE12)/D3S1400(IVH1)
882d9	840	N.D.	N.D.	D3S1394(IIIE12)/D3S1400(IVH1)
138G6	400	3p14	–	D3S1400(IVH1)
194C7	150	N.D.	N.D.	D3S1400(IVH1)
144G3	700	3p14	–	D3S1400(IVH1)
186H3	650	3p14 + D-group	+	D3S1400(IVH1)
194B5	170	N.D.	N.D.	D3S1400(IVH1)
430C2	440	3p14 + G/D-group	+	D3S1400(IVH1)
444D6	750	3p14 + D-group	+	D3S1400(IVH1)
369B2	N.D.	3p14	–	D3S1400(IVH1)
371H4	280 + 430	N.D.	N.D.	D3S1400(IVH1)
419C5	190	N.D.	N.D.	D3S1400(IVH1)
965a3	**1490**	**N.D.**	**N.D.**	**D13S1400(IVH1)/D3S1285**

Table 1. (*Continued*)

YAC	Size (kb)	Localization (by FISH)	Chimeric	DNA probe content
936g11	N.D.	N.D.	N.D.	D3S1400(IVH1)/D3S1285
811F12	**1740**	**N.D.**	**N.D.**	**D3S1285/D3S1403(VB11)/W3.2**
75H2	N.D.	3p14	–	D3S1403(VB11)
94B10	500	3p14	–	D3S1403(VB11)
376E8	N.D.	N.D.	N.D.	D3S1403(VB11)
794h5	N.D.	N.D.	N.D.	D3S1403(VB11)/W3.2
953a12	1760	N.D.	N.D.	D3S1403(VB11)/W3.2
984b9	1100	N.D.	N.D.	D3S1403(VB11)/W3.2/ D3S1404(VC4)
237B7	540	3p14	–	D3S1403(VB11)/W3.2/ D3S1404(VC4)
925e3	1800	3p14	–	D3S1403(VB11)/W3.2/D3S1404-(VC4)/D3S1437(XID11)
590G3	150	N.D.	N.D.	W3.2
934h6	N.D.	N.D.	N.D.	W3.2
838g6	N.D.	N.D.	N.D.	W3.2
838g7	N.D.	N.D.	N.D.	W3.2
900g10	N.D.	N.D.	N.D.	W3.2
901g10	N.D.	N.D.	N.D.	W3.2
902g10	N.D.	N.D.	N.D.	W3.2
238H10	400	3p14	–	W3.2/D3S1404(VC4)
446E7	440	3p14	–	W3.2/D3S1404(VC4)
625E12	N.D.	N.D.	N.D.	W3.2/D3S1404(VC4)
640C7	N.D.	N.D.	N.D.	W3.2/D3S1404(VC4)
698H8	580	3p13–p14 + 3p24 + C-group	+	W3.2/D3S1404(VC4)
6F10	350	3p13–p14	–	W3.2/D3S1404(VC4)
131H10	N.D.	N.D.	N.D.	W3.2/D3S1404(VC4)
9F1	420	3p13–p14	–	W3.2/D3S1404(VC4)
769g8	800	N.D.	N.D.	W3.2/D3S1404(VC4)/D3S1437 (XID11)/Alu578
879F9	**N.D.**	**N.D.**	**N.D.**	**W3.2/D3S1404(VC4)/ D3S1437(XID11)/ Alu578/654L**
194H11	340	3p14	–	D3S1404(VC4)
70e12	340	N.D.	–	D3S1437(XID11)/Alu578
178a3	**470**	**N.D.**	**N.D.**	**654L/D3S1217**
258b7	820	N.D.	N.D.	D3S1217
892d2	**N.D.**	**N.D.**	**N.D.**	**D3S1217/AFM289vb5**
961a9	**1460**	**N.D.**	**N.D.**	**AFM289vb5/D3S1392-(IIE2)/2H1**
89C1	375	3p13–p14	–	D3S1392(IIE2)
206B3	540 + 480	3p14	–	D3S1392(IIE2)
210H12	400	3p14 + 5q	+	D3S1392(IIE2)
277B12	340 + 250	3p14	–	D3S1392(IIE2)
372F6	350	3p14	–	D3S1392(IIE2)

Table 1. (*Continued*)

YAC	Size (kb)	Localization (by FISH)	Chimeric	DNA probe content
432D9	370	3p14	–	D3S1392(IIE2)
957d4	N.D.	N.D.	N.D.	D3S1392(IIE2)
983a5	N.D.	N.D.	N.D.	D3S1392(IIE2)/2H1
951f1	N.D.	N.D.	N.D.	D3S1392(IIE2)/2H1
393B8	350	3p14	–	D3S1392(IIE2)/2H1
932h9	1400	N.D.	N.D.	D3S1392(IIE2)/2H1/D3S1395(IVA4)/ D3S1393(IIIE1)
940f6	90	N.D.	N.D.	D3S1392(IIE2)/2H1/D3S1395(IVA4)/ D3S1393(IIIE1)
890d7	**2000**	**3p13–p14**	**–**	**D3S1392(IIE2)/2H1/D3S1395-(IVA4)/D3S1393(IIIE1)/D3S1261/2B6/D3S1398(IVD2)/D3S1399-(IVE1)/D3S1389(IA3)/D3S1296**
628E8	N.D.	N.D.	N.D.	2H1
763c3	N.D.	N.D.	N.D.	2H1
858c8	N.D.	N.D.	N.D.	2H1
616A10	870	N.D.	N.D.	D3S1395(IVA4)/D3S1393(IIIE1)
707H9	250	D-group	+	D3S1395(IVA4)/D3S1393(IIIE1)
632E4	850	3p12–p13 + p14	+	D3S1395(IVA4)/D3S1393(IIIE1)
181H6	600	3p13 + 3p14	–	D3S1395(IVA4)/D3S1393(IIIE1)
293D1	250 + 850	3p14 + 1p21 + 1p31 + C-group + G/D-group	+	D3S1395(IVA4)/D3S1393(IIIE1)
415F7	420	3p14	–	D3S1395(IVA4)/D3S1393(IIIE1)
675F12	1300	3p13–p14	+	D3S1395(IVA4)/D3S1393(IIIE1)/ D3S1261/2B6/D3S1398(IVD2)/ D3S1399(IVE1)/D3S1389(IA3)
932h2	N.D.	N.D.	N.D.	D3S1395(IVA4)/D3S1393(IIIE1)/ D3S1261/2B6/D3S1398(IVD2)/ D3S1399(IVE1)
757g3	N.D.	N.D.	N.D.	D3S1395(IVA4)/ D3S1393(IIIE1)/D3S1261
933a9	1500	N.D.	N.D.	D31261/2B6/D3S1398(IVD2)/ D3S1399(IVE1)/D3S1389(IA3)
925c9	N.D.	N.D.	N.D.	D3S1261/2B6/D3S1398(IVD2)/ D3S1399(IVE1)/D3S1389(IA3)/ D3S1296/108R/D3S1566
318G6	320	3p24–p24	–	2B6
515H4	550	C-group	+	2B6
654C5	510	C-group	+	2B6
666F7	660	N.D.	N.D.	2B6
929a9	1600	N.D.	N.D.	2B6
752f5	1390	N.D.	N.D.	2B6
966f8	N.D.	N.D.	N.D.	2B6
852e9	N.D.	N.D.	N.D.	2B6
939a3	N.D.	N.D.	N.D.	2B6
408B8	150	3p13–p14 + D-group	+	2B6/D3S1398(IVD2)

Table 1. (*Continued*)

YAC	Size (kb)	Localization (by FISH)	Chimeric	DNA probe content
248C10	400	3p13–p14 + G/D-group	+	2B6/D3S1398(IVD2)
309C11	300	3p13–p14 + G/D-group	+	2B6/D3S1398(IVD2)
169B5	280 + 400	3p13–p14	–	2B6/D3S1398(IVD2)
56C5	820	N.D.	N.D.	2B6/D3S1398(IVD2)
163A9	440	3p13–p14 + G/D-group	+	2B6/D3S1398(IVD2)
158B6	400	3p13–p14 + G/D-group	+	2B6/D3S1398(IVD2)
261C12	730	3p13–p14 + 1q	+	2B6/D3S1398(IVD2)
280G2	N.D.	N.D.	N.D.	2B6/D3S1398(IVD2)
754d9	N.D.	N.D.	N.D.	D3S1399(IEV1)/D3S1389(IA3)/ D3S1296/108R/D3S1566
90C8	410	3p14	–	D3S1389(IA3)
154D3	320	3p14	–	D3S1389(IA3)
879c2	N.D.	N.D.	N.D.	D3S1389(IA3)
765d4	**N.D.**	**N.D.**	**N.D.**	**D3S1389(IA3)/D3S1296/108R**
792d9	N.D.	N.D.	N.D.	D3S1389(IA3)/D3S1296/108R
879d2	N.D.	N.D.	N.D.	D3S1389(IA3)/D3S1296/108R
798g10	N.D.	N.D.	N.D.	D3S1389(IA3)/D3S1296/108R/ D3S1566
801a2	N.D.	N.D.	N.D.	D3S1389(IA3)/D3S1296/108R/ D3S1566
692a6	N.D.	N.D.	N.D.	D3S1389(IA3)/108R/D3S1566
942e4	N.D.	N.D.	N.D.	D3S1296/108R
943d10	N.D.	N.D.	N.D.	D3S1296/108R
957A5	N.D.	N.D.	N.D.	D3S1296/108R/D3S1566/D3S1562
762c6	N.D.	N.D.	N.D.	108R/D3S1566
791e8	N.D.	N.D.	N.D.	108R/D3S1566
914c8	N.D.	N.D.	N.D.	108R/D3S1566
853B9	N.D.	N.D.	N.D.	108R/D3S1566/D3S1562
934g10	N.D.	N.D.	N.D.	D3S1562
944B3	1640	N.D.	N.D.	108R/D3S1566/D3S1562/2A5
808B10	1500	3p14	–	D3S1566/D3S1562/2A5
808c10	N.D.	N.D.	N.D.	108R/D3S1566/D3S1562/2A5/D3S6
869d7	N.D.	N.D.	N.D.	108R/D3S1566/D3S1562/2A5/D3S6
976e4	N.D.	N.D.	N.D.	108R/D3S1566/D3S1561/2A5/D3S6
760A5	**2500**	**3p13**	**–**	**108R/D3S1566/D3S1562/2A5/ D3S6**
757H10	1000	3p13–p14	–	2A5
21D3	510	3p13–p14 + 14 or 15p	+	2A5
79C11	430	3p13–p14	–	2A5
96G1	630	3p13–p14	–	2A5
201E6	390	N.D.	N.D.	2A5
698G8	930	3p13–p14 + D-group	+	2A5
325F3	370	3p14	–	2A5

Table 1. (*Continued*)

YAC	Size (kb)	Localization (by FISH)	Chimeric	DNA probe content
869D7	1500	N.D.	N.D.	2A5
308F11	880	3p14 + others	+	D3S6/D3S1390(IA11)
884D6	**860**	**3p13–p14**	–	**2A5/D3S6**
676H5	1530	3p14	–	2A5/D3S6
976E4	1425	N.D.	N.D.	2A5/D3S6
873e10	N.D.	N.D.	N.D.	D3S6/D3S1390(IA11)/D3S30/ 2C5/D3S1405(VIG10)
940e8	**N.D.**	**N.D.**	–	**D3S1390(IA11)/D3S30/2C5/ D3S1405(VIG10)**
146F3	350	3p13–p14 + 2q23–q24	+	D3S1390(IA11)
145F3	600	2q22	+	D3S1390(IA11)
147F3	520	4q13	+	D3S1390(IA11)
148F3	410	C-group	+	D3S1390(IA11)
958c3	N.D.	N.D.	N.D.	D3S1390(IA11)
850e3	N.D.	N.D.	N.D.	D3S1390(IA11)
948a7	N.D.	N.D.	N.D.	D3S1390(IA11)
737a4	N.D.	N.D.	N.D.	D3S1390(IA11)
802D1	2000	3p12–p13	–	2C5/D3S1405(VIG10)
821C10	480	3p12–p13	–	2C5/D3S1405(VIG10)
981C11	2000	3p12–p13 + 18	+	2C5/D3S1405(VIG10)
332F8	410	3p12–p13	–	D3S1405(VIG10)
729C2	1770	3p12–p13 + 9q + 3q27–q28 + B-group	+	D3S1405(VIG10)
[gap]				
324F1	280	3p12–p13 + D-group	+	D3S1406(IIIB4)
768a5	N.D.	N.D.	N.D.	D3S1406(IIIB4)
768d12	N.D.	N.D.	N.D.	D3S1406(IIIB4)
751h12	N.D.	N.D.	N.D.	D3S1406(IIIB4)
786d4	N.D.	N.D.	N.D.	D3S1406(IIIB4)
814g3	N.D.	N.D.	N.D.	D3S1406(IIIB4)
905d2	N.D.	N.D.	N.D.	D3S1406(IIIB4)
927c4	N.D.	N.D.	N.D.	D3S1406(IIIB4)
872g3	N.D.	N.D.	N.D.	D3S1406(IIIB4)
872g10	N.D.	N.D.	N.D.	D3S1406(IIIB4)
[gap]				
376G4	N.D.	3p12	–	D3S3

YACs are listed from distal to proximal according to their position within the contig. YAC coordinates printed in boldface type belong to the minimal tiling pathway. Gaps localized to 3p12–p13 are indicated. CEPH YAC coordinates, YAC sizes, YAC localizations as detected by fluorescence in situ hybridization, and state of chimerism of YACs are given. (–) Nonchimeric; (+) chimeric; (N.D.) not done.

liable confirmation of the overlap described by Gemmill et al. (1995). Furthermore, in the contig described by Gemmill et al. (1995), YAC D20f4 contains DNA markers that also map to YAC

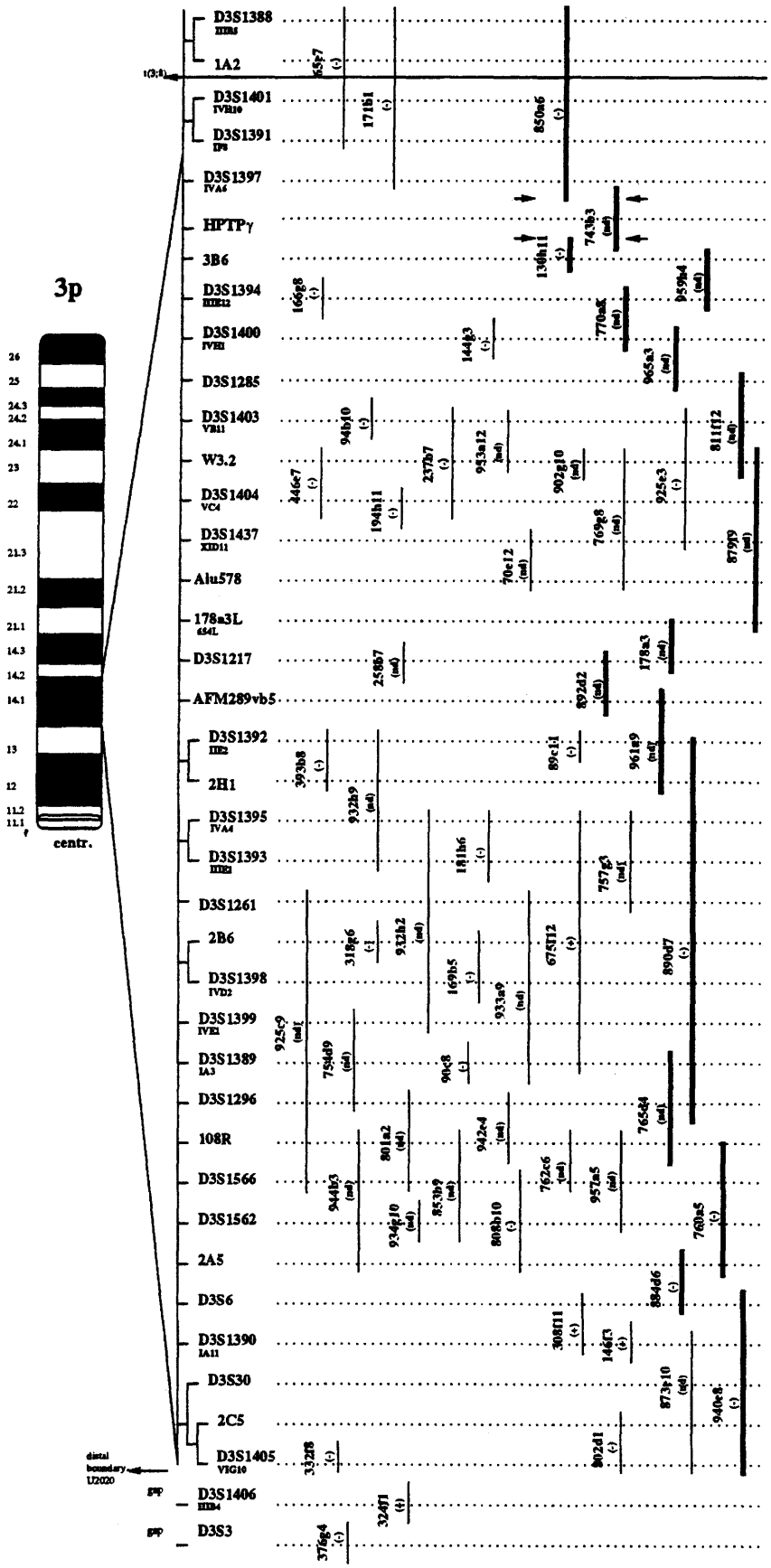

Figure 1 Contig of HCR 3p14.1. The contig consists of 171 YACs, 56 of which are shown. These were selected to define the order of DNA probes; one YAC is shown for each DNA probe combination found. The contig defines the order of 37 DNA probes including 24 STSs, the HPTPγ gene, and reference markers D3S6 and D3S30, as well as one Alu-PCR product, two YAC end probes, and seven microsatellite markers; the remaining two probes map to 3p13 and are not integrated into the contig. STSs 1A2 and D3S1388 map distal to the t(3;8) translocation breakpoint in 3p14.2. Overlaps of YACs identified by Alu-fingerprint analysis are indicated by arrows. YACs of the minimal tiling pathway spanning the entire contig are printed in bold. The state of chimerism is indicated in brackets: (−) Nonchimeric; (+) chimeric; (nd) not done. The two YACs identified with D3S1406 and D3S3 map in the U2020 deletion in 3p12–p13 and do not overlap, either with the most proximal YAC of the contig or with each other.

258b7, but none of these DNA probes map to 892d7 or 178a3. Here, we show that YAC D20f4 is chimeric: its right end probe does not map to chromosome 3, whereas its left end probe does not map to YAC 258b7 but to 3p21.1 as detected by PCR-based analysis of a hybrid mapping panel (Bardenheuer et al. 1994). Thus, the inconsistent STS content of YAC D20f4 described by Gemmill et al. (1995) could be resolved. Overall, there is no inconsistency concerning the DNA probe content of YACs for the DNA probes used in the assembly of our contig.

The overall rate of chimerism detected was 41%, which is in agreement with published data for the CEPH and other YAC libraries (Cohen et al. 1993). Because of the high redundance of our contig, it was possible to obtain nonchimeric YACs for 31 out of the 37 DNA markers contained in the contig. As there remain many YACs to be tested for chimerism by FISH, it should be possible to identify nonchimeric YACs for most if not all of these markers. These YACs may be of considerable value for functional analyses and isolation of transcribed sequences from HCR 3p14.1. Thus, in conclusion, the contig described here, together with the previously published 3p14.2–p14.3 contig may be beneficial for further investigation of this putative tumor suppressor gene region.

METHODS

Localization of STSs and Isolation of YACs

Strategy and techniques for isolation of 3p13–p14.2-specific STSs from an HCR 3p14-specific microdissection library, mapping of STSs using a deletion hybrid panel, STS-based screening of the Centre d'Etude du Polymorphisme Humain (CEPH) YAC libraries, separation of yeast chromosomes by pulsed-field gel electrophoresis (PFGE), and isolation of YAC DNA were performed as described previously (Bardenheuer et al. 1994; Michaelis et al. 1995). Isolation of YAC end probes was performed according to Riley et al. (1990), and the Alu-PCR probe was generated according to Lengauer et al. (1992). The sequences for PCR primers of microsatellite markers D3S1261, D3S1285, D3S1296, D3S1562, D3S1566, and D3S1217 were identical to those published by Gyapay et al. (1994) and Hudson et al. (1992); sequences for PCR primers of microsatellite marker AFM289vb5 were kindly provided by D. LePaslier (CEPH, Paris, France). DNA sequencing was performed using an automated DNA sequencer (A.L.F., Pharmacia Biotech, Freiburg, Germany). Southern blot analysis was performed according to standard precedures using Hybond N+ membranes (Amersham, Braunschweig, Germany) and an alkaline transfer method according to the manufacturer's recommendations.

Fluorescence In Situ Hybridization Analysis of YACs

For fluorescence in situ hybridization (FISH) analyses, total yeast DNA containing the respective YAC was used. DNA preparation, labeling of probe, suppression of repetitive sequences with Cot1 DNA, hybridization conditions, and image analyses were performed as described previously (Michaelis et al. 1995).

Contig assembly

Overlapping YAC clones were identified by PCR analyses using STS-specific primers and YAC DNA as template. All PCR analyses were preformed at least twice using the DNA of individual YAC clones as templates. Alu-fingerprinting data were obtained from the CEPH–Généthon data bank (Weissenbach et al. 1992).

ACKNOWLEDGMENTS

W.B. was supported by a fellowship from "Boehringer Ingelheim Fonds," Stuttgart, Germany; S.M. was supported by a fellowship of the Graduiertenkolleg "Normale und maligne Zellen," University of Essen, Germany; FISH analyses were supported by a European Molecular Biology Organization fellowship, Heidelberg, Germany (ASTF 7667). We thank N. Süss-Lobbermeier and Drs. G. Prescher, P. Rabbitts, and A. Heppel-Parton for valuable help with the FISH analyses. We thank D. Le Paslier and D. Cohen for providing YAC clones as well as the Alu-fingerprint data. Thanks to expert technical assistance by Birgit Todt, Ulrike Müller and Katja Schmidtke. This work was supported by Deutsche Forschungsgemeinschaft, Bonn (SFB 354).

The publication costs of this article were defrayed in part by payment of page charges. This article must therefore be hereby marked "advertisement" in accordance with 18 USC section 1734 solely to indicate this fact.

REFERENCES

Bardenheuer, W., S. Szymanski, A. Lux., H.-J. Lüdecke, B. Horsthemke, U. Claussen, G. Senger, D.I. Smith, N.-D. Wang, D. LePaslier, D. Cohen, A. Heppell-Parton, P. Rabbitts, J. Schütte, and B. Opalka. 1994. Characterization of a microdissection library from human chromosome region 3p14. *Genomics* **19:** 291–297.

Becker, D. and A.A. Sahin. 1989. Loss of heterozygosity at chromosomal regions 3p and 13q in non-small-cell carcinoma of the lung represents low frequency events. *Genomics* **4:** 97–100.

Bergerheim, U., M. Nordenskjöld and V. Collins. 1989. Deletion mapping in human renal cell carcinoma. *Cancer Res.* **49:** 1390–1396.

Boldog, F.L., R.M. Gemmill, C.M. Wilke, T.W. Glover, A.-S. Nilsson, S.C. Chandrasekharappa, R.S. Brown, F.P. Li, and H.A. Drabkin. 1993. Positional cloning of the hereditary renal carcinoma 3;8 chromosome

translocation breakpoint. *Proc. Natl. Acad. Sci.* **90:** 8509–8513.

Boldog, F.L., B. Waggoner, T.W. Glover, I. Chumakov, D. LePaslier, D. Cohen, R.M. Gemmill, and H.A. Drabkin. 1994. Integrated YAC contig containing the 3p14.2 hereditary Renal Cell Carcinoma 3;8 translocation breakpoint and the fragile site FRA3B. *Genes Chromosomes Cancer* **11:** 216–221.

Brauch, H., B. Johnson, J. Hovis, T. Yano, A. Gazdar, O. Pettengill, S. Graziano, G. Sorenson, B. Poiesz, J. Minna, M. Linehan, and B. Zbar. 1987. Molecular analysis of the short arm of chromosome 3 in small-cell and non-small-cell carcinoma of the lung. *N. Engl. J. Med.* **317:** 1109–1113.

Cohen, A.J., F.P. Li, S. Berg, D.J. Marchetto, S. Tsai, S.C. Jacobs, and R.S. Brown. 1979. Hereditary renal-cell carcinoma associated with a chromosomal translocation. *N. Engl. J. Med.* **301:** 592–595.

Cohen D., I. Chumakov, and J. Weissenbach. 1993. A first generation physical map of the human genome. *Nature* **366:** 698–701.

Devilee, P., M. van den Broek, N. Kuipers-Dijkshoorn, R. Kolluri, P. Khan, P. Pearson, and C.J. Cornelisse. 1989. At least four different chromosomal regions are involved in loss of heterozygosity in human breast carcinoma. *Genomics* **5:** 554–560.

Drabkin, H.A., C. Bradley, I. Hart, J. Bleskan, F.P. Li, and D. Patterson. 1985. Translocation of c-myc in the hereditary renal cell carcinoma associated with a t(3;8)(p14.2;q24.13) chromosomal translocation. *Proc. Natl. Acad. Sci.* **82:** 6980–6984.

Ehlen, T. and L. Dubeau. 1990. Loss of heterozygosity on chromosomal segments 3p, 6q and 11p in human ovarian carcinomas. *Oncogene* **5:** 219–223.

Gemmill, R.M., I. Chumakov, P. Scott, B. Waggoner, P. Rigault, Q, Chen, J. Weissenbach, K. Gardiner, H. Wang, Y. Pekarsky, I. Le Gall, D. Le Paslier, S. Guillou, E. Li, L. Robinson, L. Hahner, S. Todd, D. Cohen, and H.A. Drabkin. 1995. A second-generation YAC contig map of human chromosome 3. *Nature* **377:** 299–319.

Gyapay, G. J. Morissette, A. Vignal, C. Dib, C. Fizames, P. Millasseau, S. Marc, G. Bernardi, M. Lathorp, and J. Weissenbach. 1994. The 1993-94 Généthon human genetic linkage map. *Nature Genet.* **7:** 246–339.

Hibi, K., T. Takahashi, Y. Sekido, R. Ueda, T. Hida, Y. Ariyoshi, H. Takagi, and T. Takahashi. 1991. Coexpression of the stem cell factor and the c-kit genes in small-cell lung cancer. *Oncogene* **6:** 2291–2296.

Hibi, K., T. Takahashi, K. Yamakawa, R. Ueda, Y. Sekido, Y. Ariyoshi, M. Suyama, H. Takagi, Y. Nakamura, and T. Takahashi. 1992. Three distinct regions involved in 3p deletion in human lung cancer. *Oncogene* **7:** 445–449.

Hudson, T.J., M. Engelstein, M.K. Lee, E.C. Ho, M.J. Rubenfield, C.P. Adams, D.E. Housman, and N.C. Dracopoli. 1992. Isolation and chromosomal assignment of 100 highly informative human simple sequence repeat polymorphisms. *Genomics* **13:** 622–629.

Johnson, B.E., A.Y. Sakaguchi, A.F. Gazdar, J.D. Minna, D. Burch, A. Marshall, S.L. Naylor. 1988. Restriction fragment length polymorphism studies show consistent loss of chromosome 3p alleles in small cell lung cancer patients' tumors. *J. Clin. Invest.* **82:** 502–507.

Jones, M.H., S. Koi, I. Fujimoto, K. Hasumi, K. Kato, and Y. Nakamura. 1994. Allelotype of uterine cancer by analysis of RFLP and microsatellite polymorphisms: Frequent loss of heterozygosity on chromosome arms 3p, 9q, 10q and 17p. *Genes Chromosomes Cancer* **9:** 119–123.

Klingelhutz, A.J., S.-Q. Wu, J. Huang, and C.A. Reznikoff. 1992. Loss of 3p13-p21.2 in tumorigenic reversion of a hybrid between isogeneic nontumorigenic and tumorigenic human uroepithelial cells. *Cancer Res.* **52:** 1631–1634.

Kohno T., H. Takayama, M. Hamaguchi, H. Takano, N. Yamaguchi, H. Tsuda, S. Hirohashi, H. Vissing, M. Shimizu, M. Oshimura, and J. Yokota. 1993. Deletion mapping of chromosome 3p in human uterine cervical cancer. *Oncogene* **8:** 1825–1832.

Kok, K., J. Osinga, B. Carritt, M.B. Davis, A.K. van der Hout, A.Y. van der Veen, R.M. Landsvater, L.F.M.H. de Leji, H.H. Berendsen, P.E. Postmus, S. Poppema, and C.H.C.M. Buys. 1987. Deletion of a DNA sequence at the chromosomal region 3p21 in all major types of lung cancer. *Nature* **330:** 578–581.

Kovacs, G., P. Brusa, and W. de Riese. 1989. Tissue specific expression of a constitutional 3;6 translocation: Development of multiple bilateral renal cell carcinomas. *Int. J. Cancer* **43:** 422–427.

Latif, F., M. Fivash, G. Glenn, K. Tory, M. Orcutt, K. Hampsch, J. Delisio, M. Lerman, J. Cowan, M. Beckett, and R. Weichselbaum. 1992. Chromosome 3p deletions in head and neck carcinomas: Statistical ascertainment of allelic loss. *Cancer Res.* **52:** 1451–1456.

Lengauer, C., E.D. Green, and T. Cremer. 1992. Fluorescence in situ hybridization of YAC clones after Alu-PCR amplification. *Genomics* **13:** 826–828.

Lothe, R., S. Fossa, A. Stenwig, Y. Nakamura, R. White, A. Borresen, and A. Brogger. 1989. Loss of 3p or 11p alleles is associated with testicular cancer tumors. *Genomics* **5:** 134–138.

Markkanen, A., T. Ruutu, V. Ras, K. Frassila, S. Knutila, and A. de la Chapelle. 1987. Constitutional translocation t(3;6)(3p14.3;p11) in a family with hematologic malignancies. *Cancer Genet. Cytogenet.* **25:** 87–95.

Michaelis S., W. Bardenheuer, A. Lux, A. Schramm, A. Gockel, R. Siebert, C. Willers, K. Schmidtke, B. Todt,

A.H. van der Hout, H.C.M.C. Buys, A. Heppell-Parton, P. Rabbitts, D.I. Smith, D. LePaslier, D. Cohen, B. Opalka, and J. Schütte. 1995. Characterization and chromosomal assignment of yeast artificial chromosomes containing human 3p13-p21-specific sequence tagged sites. *Cancer Genet. Cytogenet.* **81:** 1–12.

Mori, N., J. Yokota, and M. Oshimura. 1989. Concordant deletions of chromosome 3p and loss of heterozygosity for chromosomes 13 and 17 in small cell lung carcinoma. *Cancer Res.* **49:** 5130–5135.

Morita, R., J. Ishikawa, M. Tutsumi, K. Hikiji, Y. Tsukada, S. Kamidono, S. Maeda, and Y. Nakamura. 1991. Allelotype of renal cell carcinoma. *Cancer Res.* **51:** 820–823.

Naylor, S., B. Johnson, J. Minna, and A. Sakaguchi. 1987. Loss of heterozygosity of chromosome 3 markers in small-cell lung cancer. *Nature* **329:** 451–454.

Rabbitts P., J. Douglas, M. Daly, V. Sundaresan, B. Fox, P. Haselton, F. Wells, D. Albertson, J. Waters, and J. Bergh. 1989. Frequency and extent of allelic loss of the short arm of chromosome 3 in nonsmall-cell lung cancer. *Genes Chromosomes Cancer* **1:** 95–105.

Riley, J., R. Butler, D. Ogilvie, R. Finniear, D. Jenner, S. Powell, R. Anand, J.C. Smith, and A.F. Markham. 1990. A novel, rapid method for the isolation of terminal sequences from yeast artificial chromosome (YACs) clones. *Nucleic Acids Res.* **18:** 2887–2890.

Sanchez, Y., A. El-Naggar, S. Pathak, and A.M.N. Killary. 1994. A tumor suppressor locus within 3p14-p12 mediates rapid cell death of renal cell carcinoma in vivo. *Proc. Natl. Acad. Sci.* **91:** 3383–3387.

Sato, T., F. Akiyama, G. Sakamoto, F. Kasumi, and Y. Nakamura. 1991. Accumulation of genetic alterations and progression of primary breast cancer. *Cancer Res.* **51:** 5794–5799.

Smith, S.E., A. Joseph, S. Nadeau, V. Shridhar, R. Gemmill, H. Drabkin, S. Knuutila, and D.I. Smith. 1993. Cloning and characterization of the human t(3;6)(p14;p11) translocation breakpoint associated with hematologic malignancies. *Cancer Genet. Cytogenet.* **71:** 15–21.

Trent, J., F. Thompson, and R. Buick. 1985. Generation of clonal variants in a human ovarian carcinoma studied by chromosome banding analysis. *Cancer Genet. Cytogenet.* **14:** 153–161.

van den Berg, A., A.Y. van der Veen, M.M.F. Hulsbeek, G. Kovacs, R.M. Gemmill, H.A. Drabkin, and C.H.C.M. Buys. 1995. Defining the position of the breakpoint of the constitutional t(3;6) occurring in a family with renal cell carcinoma. *Genes Chromosomes Cancer* **12:** 224–228.

Wang, N. and K.L. Perkins. 1984. Involvement of band 3p14 in t(3;8) hereditary renal carcinoma. *Cancer Genet. Cytogenet.* **11:** 479–481.

Weissenbach, J., G. Gyapay, C. Dib, A. Vignal, J. Morissette, P. Millasseau, G. Vaysseix, and M. Lathrop. 1992. A second-generation linkage map of the human genome. *Nature* **359:** 794–801.

Weston, A., J. Willey, R. Modali, H. Sugimura, E. McDowell, J. Resau, B. Light, A. Haugen, D. Mann, B. Trump, and C. Harris. 1989. Differential DNA sequence deletions from chromosomes 3, 11, 13, and 17 in squamous-cell carcinoma, large-cell carcinoma, and adenocarcinoma of the lung. *Proc. Natl. Acad. Sci.* **86:** 5099–5103.

Whang-Peng, J., T. Knutsen, E. Douglass, E. Chu, R. Ozols, W. Hogan, and R. Young. 1984. Cytogenetic studies in ovarian cancer. *Cancer Genet. Cytogenet.* **11:** 91–106.

Wilhelm, M., P. Bugert, C. Kenk, G. Staehler, and G. Kovacs. 1995. Terminal deletion of chromosome 3p sequences in nonpaillary renal cell carcinomas: A breakpiont cluster between loci *D3S1285* and *D3S1603*. *Cancer Res.* **55:** 5383–5385.

Yokoyama, S., K. Yamakawa, E. Tsuchiya, M. Murata, S. Sekiyama, and Y. Nakamura. 1992. Deletion mapping on the short arm of chromosome 3 in squamous cell carcinoma and adenocarcinoma of the lung. *Cancer Res.* **52:** 873–877.

Yokota, J., M. Wada, Y. Shimosato, M. Terada, and T. Sugimura. 1987. Loss of heterozygosity on chromosomes 3, 13, and 17 in small-cell carcinoma and on chromosome 3 in adenocarcinoma in the lung. *Proc. Natl. Acad. Sci* **84:** 9252–9256.

Yokota J., Y. Tsukada, T. Nakajima, M. Gotoh, Y. Shimosato, N. Mori, Y. Tsunokawa, T. Sugimura, and M. Terada. 1989. Loss of heterozygosity on the short arm of chromosome 3 in carcinoma of the uterine cervix. *Cancer Res.* **48:** 2858–2866.

Zbar, B., H. Brauch, C. Talmadge, and M. Linehan. 1987. Loss of alleles of loci on the short arm of chromosome 3 in renal cell carcinoma. *Nature* **327:** 721–724.

Received July 31, 1995; accepted in revised form February 15, 1996.

Construction of a consistent YAC contig for human chromosome region 3p14.1.

W Bardenheuer, S Michaelis, A Lux, et al.

Genome Res. 1996 6: 176-186
Access the most recent version at doi:10.1101/gr.6.3.176